



Characterization and Analysis of Aerosol Particle Retention and Re-aerosolization from Hook-and-Loop Fasteners on the International Space Station

Barbara Boyajian
University of Southern California, Los Angeles, California

Marit E. Meyer
Glenn Research Center, Cleveland, Ohio

NASA STI Program . . . in Profile

Since its founding, NASA has been dedicated to the advancement of aeronautics and space science. The NASA Scientific and Technical Information (STI) Program plays a key part in helping NASA maintain this important role.

The NASA STI Program operates under the auspices of the Agency Chief Information Officer. It collects, organizes, provides for archiving, and disseminates NASA's STI. The NASA STI Program provides access to the NASA Technical Report Server—Registered (NTRS Reg) and NASA Technical Report Server—Public (NTRS) thus providing one of the largest collections of aeronautical and space science STI in the world. Results are published in both non-NASA channels and by NASA in the NASA STI Report Series, which includes the following report types:

- **TECHNICAL PUBLICATION.** Reports of completed research or a major significant phase of research that present the results of NASA programs and include extensive data or theoretical analysis. Includes compilations of significant scientific and technical data and information deemed to be of continuing reference value. NASA counter-part of peer-reviewed formal professional papers, but has less stringent limitations on manuscript length and extent of graphic presentations.
- **TECHNICAL MEMORANDUM.** Scientific and technical findings that are preliminary or of specialized interest, e.g., “quick-release” reports, working papers, and bibliographies that contain minimal annotation. Does not contain extensive analysis.
- **CONTRACTOR REPORT.** Scientific and technical findings by NASA-sponsored contractors and grantees.
- **CONFERENCE PUBLICATION.** Collected papers from scientific and technical conferences, symposia, seminars, or other meetings sponsored or co-sponsored by NASA.
- **SPECIAL PUBLICATION.** Scientific, technical, or historical information from NASA programs, projects, and missions, often concerned with subjects having substantial public interest.
- **TECHNICAL TRANSLATION.** English-language translations of foreign scientific and technical material pertinent to NASA's mission.

For more information about the NASA STI program, see the following:

- Access the NASA STI program home page at <http://www.sti.nasa.gov>
- E-mail your question to help@sti.nasa.gov
- Fax your question to the NASA STI Information Desk at 757-864-6500
- Telephone the NASA STI Information Desk at 757-864-9658
- Write to:
NASA STI Program
Mail Stop 148
NASA Langley Research Center
Hampton, VA 23681-2199



Characterization and Analysis of Aerosol Particle Retention and Re-aerosolization from Hook-and-Loop Fasteners on the International Space Station

Barbara Boyajian
University of Southern California, Los Angeles, California

Marit E. Meyer
Glenn Research Center, Cleveland, Ohio

National Aeronautics and
Space Administration

Glenn Research Center
Cleveland, Ohio 44135

Acknowledgments

The authors would like to thank Anita Garg for TEM and STEM imaging support, Daniel Gotti for VelcroBot design assistance, and the Life Support Systems Project for providing the Microgravity Science Glovebox stray-light cover.

Trade names and trademarks are used in this report for identification only. Their usage does not constitute an official endorsement, either expressed or implied, by the National Aeronautics and Space Administration.

Level of Review: This material has been technically reviewed by technical management.

Available from

NASA STI Program
Mail Stop 148
NASA Langley Research Center
Hampton, VA 23681-2199

National Technical Information Service
5285 Port Royal Road
Springfield, VA 22161
703-605-6000

This report is available in electronic form at <http://www.sti.nasa.gov/> and <http://ntrs.nasa.gov/>

Characterization and Analysis of Aerosol Particle Retention and Re-aerosolization from Hook-and-Loop Fasteners on the International Space Station

Barbara Boyajian
University of Southern California
Los Angeles, California 90007

Marit E. Meyer
National Aeronautics and Space Administration
Glenn Research Center
Cleveland, Ohio 44135

Summary

The extensive use of hook-and-loop fasteners aboard the International Space Station (ISS) contributes to indoor air pollution, as the fine fibers catch aerosol particles and then re-aerosolize them upon being pulled apart, often within the breathing zone of astronauts. This problem is expanded by the lack of gravity, because airborne particles larger than 1 μm do not settle. Instead, these aerosols remain in the air until removed by filtration. This study characterizes the size distribution, number concentration, and mass concentration of re-aerosolized debris generated by hook-and-loop fasteners taken from the stray-light cover of the Microgravity Science Glovebox in the U.S. Laboratory of the ISS to understand the extent of its impact on air quality. Transmission electron microscopy (TEM) and scanning transmission electron microscopy (STEM), in conjunction with energy-dispersive x-ray spectroscopy, were also used to characterize the morphology and composition of the particles.

Acronyms

CMC	Cargo Mission Contract
CMD	count median diameter
EDS	energy-dispersive x-ray spectroscopy
FGB	Functional Cargo Block
GSD	geometric standard deviation
HAADF	high-angle annular dark field
HEPA	high-efficiency particulate air
ISS	International Space Station
MSG	Microgravity Science Glovebox
SE	standard error
SEM	scanning electron microscopy
STEM	scanning transmission electron microscopy
TEM	transmission electron microscopy
UV	ultraviolet
WCPC	water condensation particle counter

Introduction

The International Space Station (ISS) relies heavily on hook-and-loop fasteners, commercially known as VELCRO® (Velcro Companies) fasteners, to hold down objects that may float away in zero gravity. The loops, or pile, of the fasteners are affixed to the walls while the hooks, or teeth, are attached to the object to be secured. Dust normally present in any indoor environment can become embedded in the hook-and-loop material and can be re-aerosolized when the hooks and loops are pulled apart. This re-aerosolizing of retained debris increases the particle concentrations in the spacecraft cabin, and the lack of gravity prevents the settling of larger particles. As a result, aerosol particles remain in the cabin air volume until captured by a filter, deposited on walls, or breathed in by an astronaut. This experiment was conducted to characterize particles re-aerosolized by hook-and-loop fasteners to better understand their impact on the spacecraft cabin environment.

A piece of flight hardware, a stray-light cover, was retired from the ISS and returned to Earth in 2013 in the SpaceX-2 cargo vehicle. During its time aboard the ISS, the stray-light cover had been placed over the Microgravity Science Glovebox (MSG) in the U.S. Destiny module during experiments that were light sensitive or required dark conditions for optimal data collection (Figure 1) (Ref. 1). The stray-light cover was used by astronauts during many different experiments in the MSG. Therefore, the particles embedded in the hook-and-loop fasteners used on the MSG are expected to have originated from astronauts, equipment, and materials that were manipulated in the vicinity of the MSG. Subsequent stray-light covers have been used over the MSG during the ultraviolet (UV) decontamination that is performed between life science experiments, but the stray-light cover used in this experiment was not exposed to UV radiation. Although the entire storage condition history was not documented, it is assumed that the stray-light cover remained in its bag after returning to Earth until it was tested in these experiments. The returned stray-light cover had a total of 82.75 cm² of hook-and-loop material with intact and connected pairs of hook-and-loop tape segments. The stray-light cover was stored in plastic after its return to Earth, and undisturbed pairs of hook-and-loop tape were removed for use in this experiment. Aerosols that originated from the ISS can be generated on Earth by opening and closing the returned hook-and-loop fasteners.

Maintaining good air quality aboard the ISS is important for a healthy astronaut crew and mission success. The current ISS particulate matter requirement states that for missions longer than 14 days, the particulate mass concentration for particle sizes from 10 to 100 µm must be <3 mg/m³ and the respirable fraction of the dust (considered to be particle sizes from 0.5 to 10 µm aerodynamic diameter) must be <1 mg/m³ (Ref. 2). It is currently unknown if the particle mass concentration requirement is being met, as there is no measurement capability. These targets and those pertaining to permissible levels of microbial contamination are comparable to a class 100,000 clean room standard, which is met (by design) with stringent high-efficiency particulate air (HEPA)-level filtration requirements (Ref. 3). This requirement presents two size-segregated mass concentrations, which do not account for differences in health effects of ultrafine particles and high number concentrations. A high number of very fine particles can have the same mass concentration as several large particles, and the health effects on human beings can be very different.

Previous studies on airborne debris in the ISS were based on the analysis of samples returned to Earth. At Marshall Space Flight Center, contents of a HEPA vacuum cleaner bag and a piece of Functional Cargo Block (FCB) panel fabric were classified by mass and analyzed with optical microscopy and scanning electron microscopy (SEM) methods. This study focused on larger debris such as hair, lint, food, plastics, and residues with sizes ranging from 53 to 500 µm (Ref. 4). An inventory of sources of aerosol emissions was updated in 2014 in a study conducted at the NASA Glenn Research Center (Ref. 5). The chemical signatures derived from the study conducted at the Marshall Space Flight Center, as well as the updated aerosol inventory, set the expectations for what may be embedded in the hook-and-loop fibers. This study improves upon the current knowledge base regarding the air quality on the ISS by quantifying aerosol particles embedded in the hook-and-loop segments from the stray-light

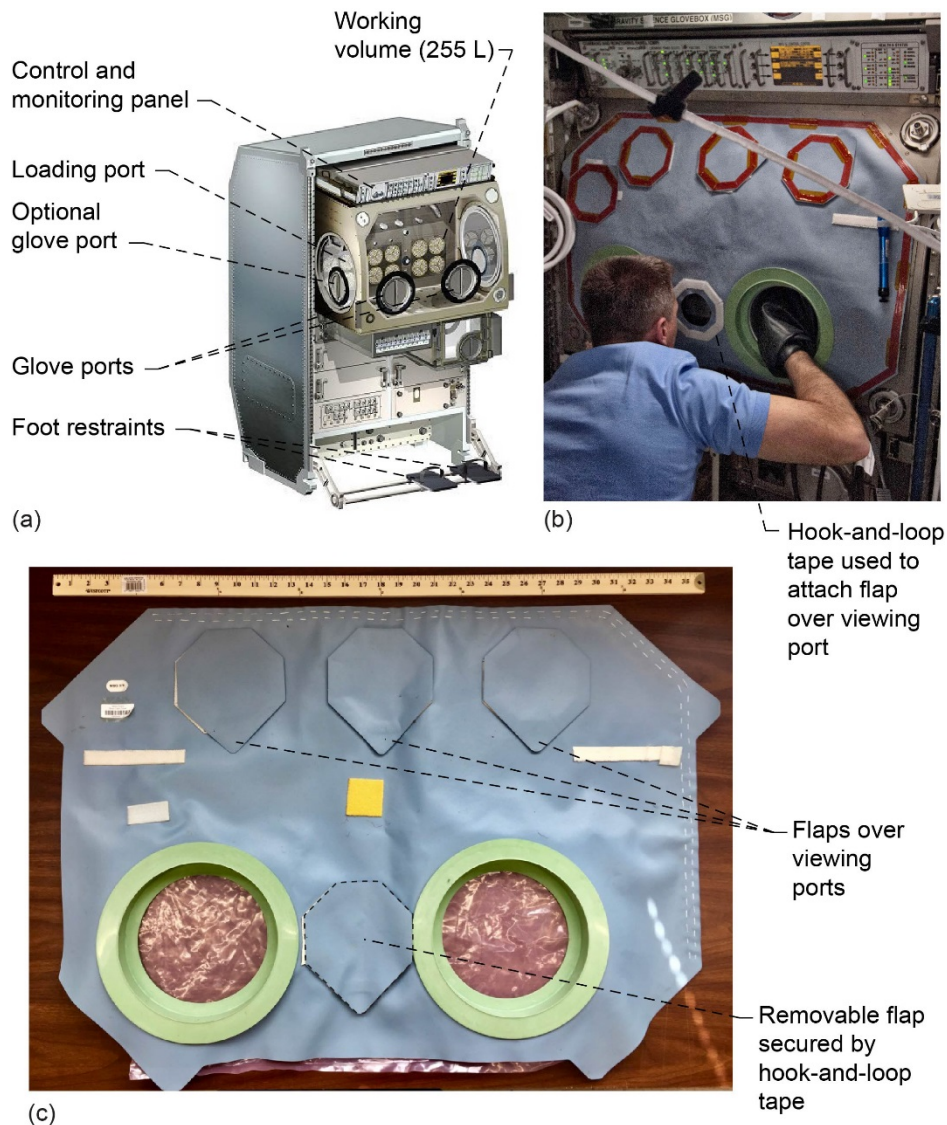


Figure 1.—Microgravity Science Glovebox (MSG). (a) Schematic. (b) In use aboard International Space Station (ISS) with stray-light cover. Hook-and-loop tape surrounds the viewing port through which the astronaut is looking. (c) ISS hook-and-loop samples were taken from this stray-light cover's removable flaps.

cover, which are re-aerosolized by mating and demating the hook-and-loop pairs. Characterizing these re-aerosolized particles is an important addition to the sparse data available on ISS particulate matter.

In this study, aerosol particles expelled by the hook-and-loop fasteners upon mating and demating were characterized in terms of mass concentration, number concentration, and particle diameter. Particle morphology and composition were also explored using electron microscopy techniques and energy-dispersive x-ray spectroscopy (EDS). Of interest was learning whether hook-and-loop fasteners emitted their own particles in addition to the embedded debris.

Methods

Four sets of hook-and-loop fasteners were used on the stray-light cover to fasten flaps over viewing ports, along with several exposed strips along the sides (Figure 1(b)). The fastener strips were removed

from the MSG stray-light cover, and only samples with intact pairs of hooks and loops were used for this study. Although the storage history is not documented, it is likely that the hook-and-loop fasteners used for this experiment were never separated after return to Earth, and therefore it is assumed that no new debris was introduced into the fasteners on the ground. However, the factory conditions in which the material was fabricated are not known, and no brand-new sample of identical hook-and-loop material was available for a control experiment.

Each sample set included the hook section and its corresponding loop pile glued onto separate wooden dowels with a diameter of 3.18 cm (Figure 2(b)). The diameter of each dowel increased to 3.45 cm when the hook-and-loop components were glued on. The hook-and-loop material on each dowel had a surface area of 6.90 cm². The samples were mounted onto two clamping shaft collars, which were fastened onto the shafts of the machine named VelcroBot (Figure 2(a)). The machine was built and designed for this experiment to rotate the hook-and-loop portions in opposite directions in a chamber that can be purged to a nearly particle-free state. Because the speed and rhythm of demating influences the amount of debris that is expelled from the fasteners, these parameters were controlled with the VelcroBot, which provided continuous mating and demating at a constant speed for all runs, increasing the repeatability of the hook-and-loop emissions. The VelcroBot uses a direct current motor and its speed is controlled with a potentiometer (Figure 2(c)). For all runs, the rotation was kept constant at 240 rpm, corresponding to a linear speed of 43.2 cm/s, to replicate a typical speed at which hook-and-loop fasteners are demated by hand as measured in the laboratory. Essentially, the VelcroBot mimicked constant-rate mating and demating of 118.06 cm² of hook-and-loop pairs per second. Other methods of opening and closing hook-and-loop fasteners may create different emission patterns; however, this method was designed to ensure repeatability with a realistic aerosol signature.

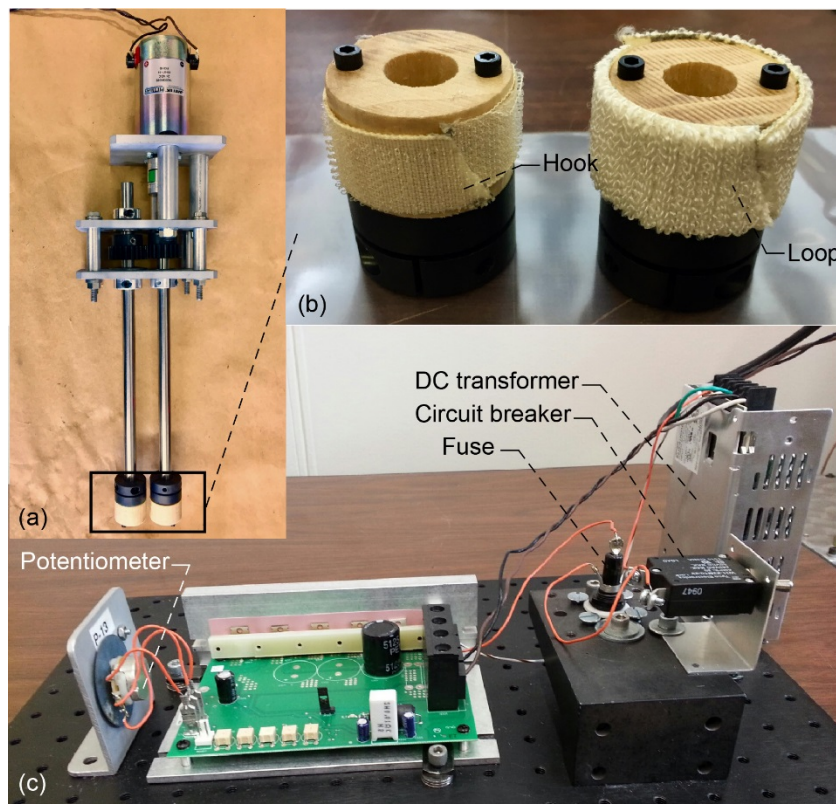


Figure 2.—Experimental test components. (a) VelcroBot (b) Hook-and-loop sample set. (c) VelcroBot hardware.

The VelcroBot was designed to be mounted in a chamber with a set of two steel tension rods. The 326-L acrylic-glass chamber used for the experiment was a repurposed glovebox, typically used as a smoke chamber for spacecraft fire safety testing. There was some residue on the walls from previous smoke experiments, which generated a relatively consistent low level of aerosol concentration. Before the fastener testing, the glovebox was wiped down several times with residue-free Alconox® (Alconox, Inc.) detergent diluted to 1 percent. The floor of the glovebox was also covered by a clean plastic sheet. The effectiveness of the cleaning was ensured by monitoring the particle number concentration with a water condensation particle counter (WCPC), TSI® (TSI Inc.) model 3787. Once the number concentration was maintained overnight at 20 particles/cm³, the glovebox was pronounced free of smoke residue. Before cleaning, the number concentration at rest inside the glovebox was 500 particles/cm³, and with every subsequent cleaning session, the variability and magnitude of the number concentrations decreased until the 20 particles/cm³ value was reached and maintained.

Tygon® (Saint-Gobain Corp.) flexible polymer tubing connected the external aerosol instruments to the chamber air through airtight feedthroughs, and a vent hatch installed on the lid of the glovebox was used for purging. After each test, aerosols were cleared from the glovebox by shop air that flowed continually through HEPA capsules into the chamber and out the hatch before being vented out of the building. The purging progress was monitored with the WCPC, and purging continued until the reading from the WCPC was below 0.8 particles/cm³ of aerosol particles. When this number concentration was reached and maintained for several minutes, the glovebox air was considered clean for the hook-and-loop experiments.

Once the purge was completed, the clean-air valve was shut off, and the vent hatch was closed prior to the test. The aerosol instruments were turned on, followed by the VelcroBot, which was loaded with a set of hook-and-loop dowels. Four instruments sampled aerosols from the chamber during tests: the WCPC (TSI® model 3787), a laser aerosol spectrometer (Las-X II®, Particle Measuring Systems®), a nephelometer (MicroPEM™, RTI), and a thermophoretic aerosol sampler that was modified for NASA (TPS100™, RJ Lee Group). (Ref. 6). The WCPC measured number concentration (particles per cm³) with a 0.6-L/min flow rate. The laser aerosol spectrometer measured the particle size distribution from 100 nm to 10 µm and sampled every 10 s for 5 min with a 1-L/min flow rate. The nephelometer recorded mass concentration data (µg/cm³) every 10 s for 5 min with a 0.5-L/min flow rate. The TPS100™ used thermophoresis as its collection method, whereby a 0.005-L/min flow deposits aerosols onto a nickel transmission electron microscopy (TEM) grid. The combined flow rate of the instruments was only 2.105 L/min, which removed only 0.6 percent of the total volume of the air in the glovebox every minute. This prevented dilution from affecting number concentration and mass concentration data. This also matches the average tidal volume of an adult male and adult female under light exercise conditions so that every 10 s of data is analogous to the volume of air inhaled by an average adult over 1 min (Ref. 7). The TPS100™ was placed in the glovebox, while the WCPC and MicroPEM™ instruments relied on 50.8 cm of a combination of conductive and nonconductive tubing and a funnel to optimize the sampling efficiency of particles, and the laser aerosol spectrometer used 182.88 cm of conductive tubing (to minimize electrostatic losses). The percent loss of particles smaller than 10 µm was calculated to be 0.3 percent due to diffusion and 4 percent due to the curvature in the tube for the WCPC and the MicroPEM™ nephelometer. For the laser aerosol spectrometer, loss due to diffusion of particles less than 10 µm was 0.11 percent and loss from gravitational settling was 0.002 percent. An image of the experimental setup is provided in Figure 3. Each hook-and-loop sample set was rotated by the VelcroBot for a period of 5 min with 14 sets tested three times each for a total of 42 trials in a randomized test matrix.

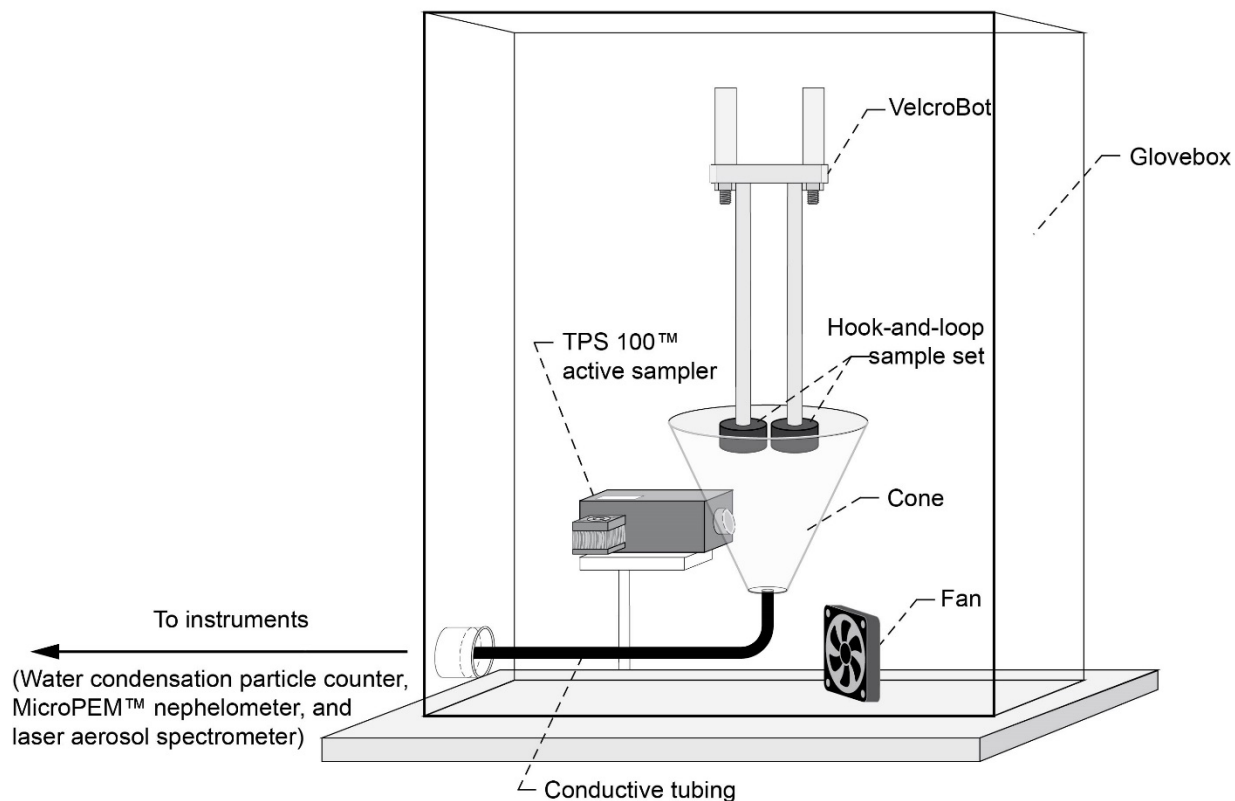


Figure 3.—Experimental test setup.

Preliminary trials with the VelcroBot were conducted to prove the viability of the experimental procedure. The WCPC was the instrument of choice in these tests due to its ability to detect particles as small as 5 nm. Preliminary tests were done to ensure that the VelcroBot itself did not produce its own aerosols in significant quantities. The test chamber was purged of aerosols, and the VelcroBot was powered on without a sample set attached. There was little difference in the WCPC measurements from the purged chamber with a motionless VelcroBot and the measurements taken while the VelcroBot was rotating over a total of three trials. Number concentration measured in the glovebox with and without turning on the machine is shown in Figure 4. The mean change in number concentration in the glovebox before running the VelcroBot was 4.03 ± 1.9 particles/cm³ ($x \pm s$). During the time the VelcroBot was running, the mean change in number concentration was 4.13 ± 2 particles/cm³ ($x \pm s$), which shows that the machine's aerosol contribution is negligible.

Another preliminary test to optimize aerosol sampling efficiency measured the radius over which the VelcroBot aerosols would settle. A set of flight hook-and-loop material was rolled in cornstarch and the deposition pattern from VelcroBot rotations was observed. The majority of the cornstarch particles fell within a radius of 13.97 cm around the VelcroBot, covering 677.42 cm². Upon closer inspection, a fine dusting of cornstarch was seen at the edges of the chamber, covering the 74.93 by 55.88-cm base. To maximize sampling efficiency of aerosols, a cone funnel was fabricated to direct VelcroBot aerosols into a segment of nonconductive tubing through which most of the instruments sampled from the glovebox. After the cone funnel was in place, more testing was done with the cornstarch-loaded hook-and-loop set to confirm the collection efficiency of the cone. The maximum number concentration registered without the cone was 1.8 particles/cm³. With the cone in place, the number concentration jumped to 93.9 particles/cm³. The higher number concentration of particles captured demonstrated that the cone increased sampling efficiency for the hook-and-loop emissions.

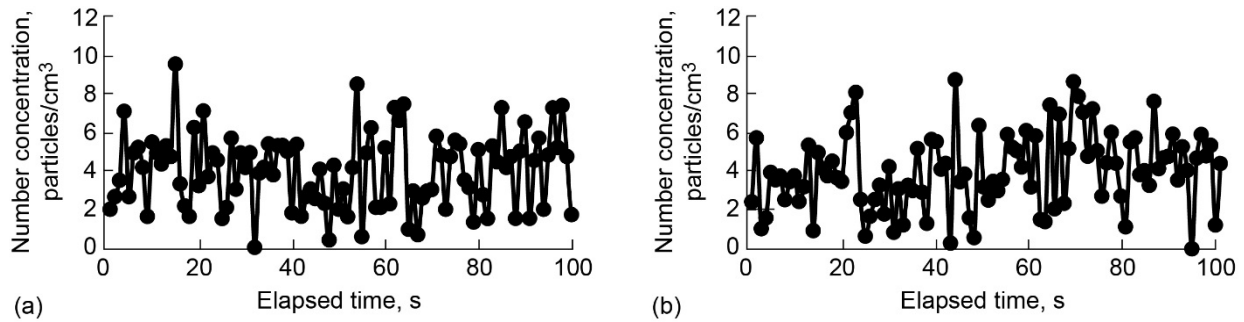


Figure 4.—Glovebox number concentration measurements. (a) Without VelcroBot rotating. (b) With VelcroBot rotating.

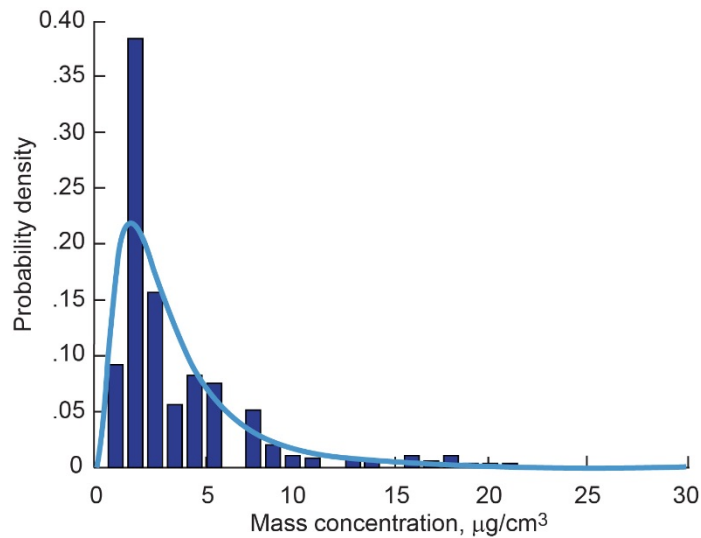


Figure 5.—Mass concentration ($\mu\text{g}/\text{cm}^3$) data from MicroPEM™ nephelometer represented as probability density distribution and its corresponding probability density function curve fit.

Results

Mass Concentration

The MicroPEM™ nephelometer produced time-dependent data of mass concentration for particles smaller than $2.5\ \mu\text{m}$ in units of $\mu\text{g}/\text{cm}^3$. The mass concentration varied over the course of each 5-min test. Rather than reporting a mean or maximum concentration for each run, a statistical analysis was performed on all MicroPEM™ data points collected. The mass concentration was binned into units of $1\ \mu\text{g}/\text{cm}^3$ and converted into a probability density distribution using MATLAB® (The MathWorks, Inc.). The instrument was experiencing issues with data acquisition, so 17 runs were lost as a result of instrument error. The probability density distribution of mass concentration from the hook-and-loop fasteners is shown in Figure 5.

It was found that 50 percent of the time, the mass concentration of the debris being expelled was less than $4.25\ \mu\text{g}/\text{cm}^3$ with a variance of $13.32\ \mu\text{g}/\text{cm}^3$. The highest peak value observed was $30.97\ \mu\text{g}/\text{cm}^3$, and the standard arithmetic mean of the peak values of all runs was $15.98 \pm 8.0\ \mu\text{g}/\text{cm}^3$ ($x \pm s$). The mass concentration on the ISS would vary from these numbers, as the free air volume in a module is significantly different from the chamber volume.

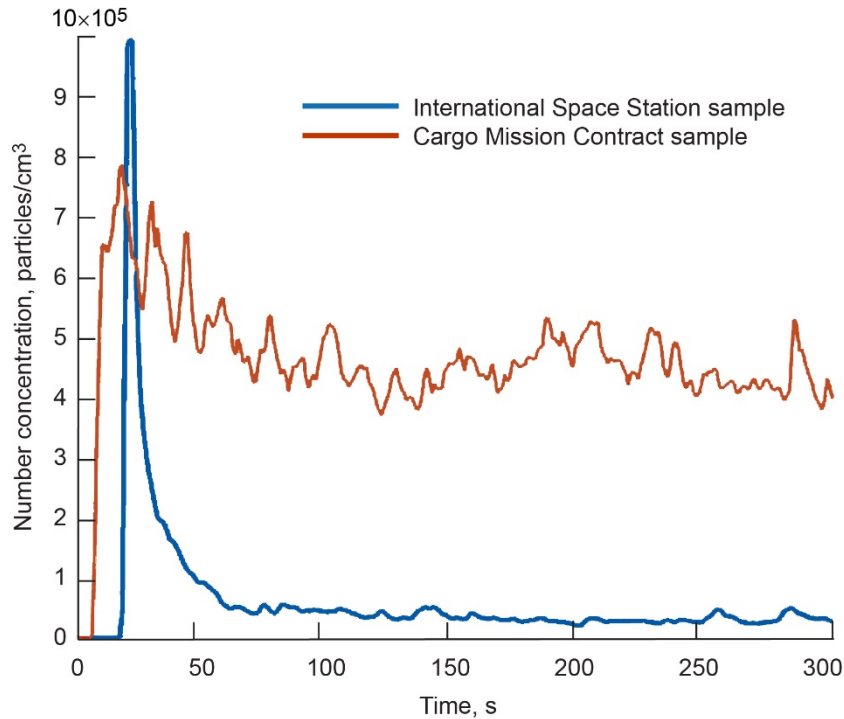


Figure 6.—Number concentration of International Space Station hook-and-loop sample and debris-free Cargo Mission Contract sample. Typical particle emission patterns observed with the two different samples are shown.

Number Concentration

Number concentration for the hook-and-loop samples varied with time, as shown in Figure 6. A similar statistical approach was taken to characterize emissions beyond the peak or average values of each run. The WCPC instrument had a sampling rate of 1 s and therefore produced 300 data points per 5-min run. Data were binned every 2,000 units for a total of 500 bins, and the frequency was plotted.

The number concentration data were designated according to the number of VelcroBot uses (e.g., samples run the first, second, or third time, or runs 1, 2, and 3) in order to consider whether the ISS debris emissions from each hook-and-loop fastener set were diminishing with each subsequent test. The WCPC can detect particles in the range of 5 nm to 3 μm. Particles binned from 0 to 2,000 particles/cm³ were disregarded, as it took several seconds to turn on all the instruments and the VelcroBot. When the VelcroBot began to rotate, the concentration that corresponded with its start time was always greater than 3,000 particles/cm³. Furthermore, most of the data in the 0 to 2,000 particles/cm³ bin were less than 1 particle/cm³, which is characteristic of the glovebox air after purging. The three runs had 14 trials each for a total of 42 as the total data set. For each run, the bin totals of all 14 trials were averaged and rounded to the nearest integer to produce a characteristic average frequency distribution. These distributions were plotted as probability density distributions (Figure 7). All three runs from the ISS samples demonstrated a skewed nature because the time-dependent data always began with a large initial spike followed by a period of exponential decline (Figure 6).

Number concentration data are summarized in Table I. The overall trend of declining mean number concentration appears to indicate that the debris in the sample is being removed with each successive run. However, the trend is not statistically significant.

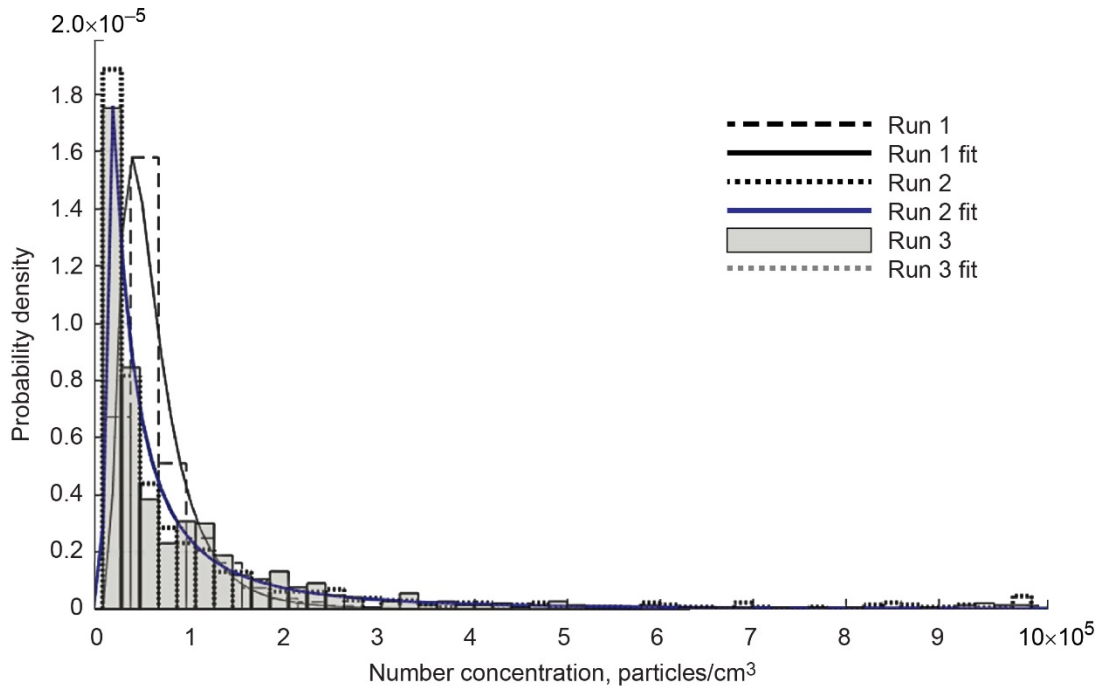


Figure 7.—Probability density distributions of number concentration for all three runs of International Space Station hook-and-loop samples.

TABLE I.—PARTICLE NUMBER CONCENTRATION DATA FOR HOOK-AND-LOOP SAMPLES
[ISS^a samples compared with CMC^b sample.]

Parameter	ISS Run 1	ISS Run 2	ISS Run 3	CMC
Number concentration, particles/cm ³				
Mean (\bar{x})	59,200	51,100	47,200	277,400
Standard error (SE)	11,500	11,600	13,900	36,100
Maximum	1×10^6	10^6	10^6	322,280
Steady state	$4.5 \times 10^4 \pm 9 \times 10^3$	$3.1 \times 10^4 \pm 7 \times 10^3$	$2.6 \times 10^4 \pm 2 \times 10^3$	$2.18 \times 10^5 \pm 2 \times 10^4$
Normal parameter fit number concentration, particles/cm ³				
($\mu \pm SE$)	10.8 ± 0.04	10.5 ± 0.05	10.4 ± 0.06	277,400
($\sigma \pm SE$)	0.7 ± 0.03	0.9 ± 0.04	0.9 ± 0.04	36,100

^aInternational Space Station

^bCargo Mission Contract

Although no brand-new equivalent of the type of hook-and-loop fasteners used on the ISS was available for comparison, some measurements were taken with a sample set made of clean, debris-free flight hook-and-loop fasteners taken from the extra inventory of the Aerosol Sampling Experiment, which was aboard the ISS in December 2016. This is the same type of material that is currently supplied to ISS payloads by Cargo Mission Contract (CMC) at Johnson Space Center. The stray-light cover fasteners were of a different construction than the comparable CMC sample and were likely made of a different material. The debris-free CMC sample was more plastic-like in appearance, and its loops were more densely packed than the more fabric-like loops of the ISS test samples. Data from the brand-new CMC samples were also converted into a probability density distribution (Figure 8). The mean number concentration of the debris-free CMC sample data was 277,400 particles/cm³ with a standard deviation of

36,100 units. The mean number concentration from the debris-free CMC sample is much higher than the test samples; this is likely a result of the nature of the material itself. While the numbers are not valid for comparison as a control due to material differences, the pattern of distributed number concentrations indicates that the CMC sample's aerosol number concentration frequency is normally distributed. In contrast, the probability distributions for the ISS samples are skewed. To evaluate the ISS test sample distributions' divergence from normality, the test sample data from all three runs were converted to the log10 scale and plotted. The goodness of fit R^2 coefficient for each run was calculated to be 0.59, 0.76, and 0.80, respectively. As each sample was tested, the distribution of aerosols emitted became increasingly skewed and diverged from a normal distribution of number concentrations.

The debris-free CMC sample reached a steady-state value within the first 10 s of testing and oscillated about that value for the remainder of the test (Figure 7), which accounts for the normal appearance of the probability density distribution. The ISS samples, however, had a much larger peak with a steady decay, representative of the very wide distribution of number concentration values (Figure 7). In summary, the CMC sample had a higher steady-state emission value than the ISS test sample, but a lower initial peak compared with the ISS test sample.

Considering that the mean number concentration does not significantly differ from run to run and the data are increasingly diverging from the normal distribution, it is possible that debris is still being expelled from the sample by the third run. In addition, when the number concentration data and mass concentration data are observed together, the high number concentrations and low mass concentrations indicate that the aerosols emitted from the test samples are very small in size.

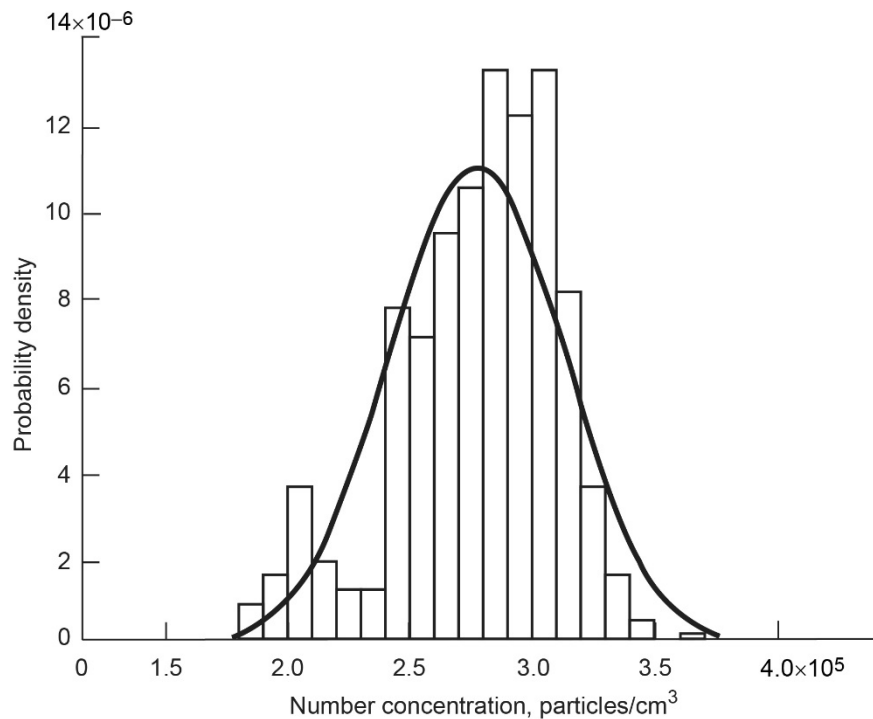


Figure 8.—Number concentration probability density distribution data and curve fit of debris-free flight hook-and-loop sample from Cargo Mission Contract.

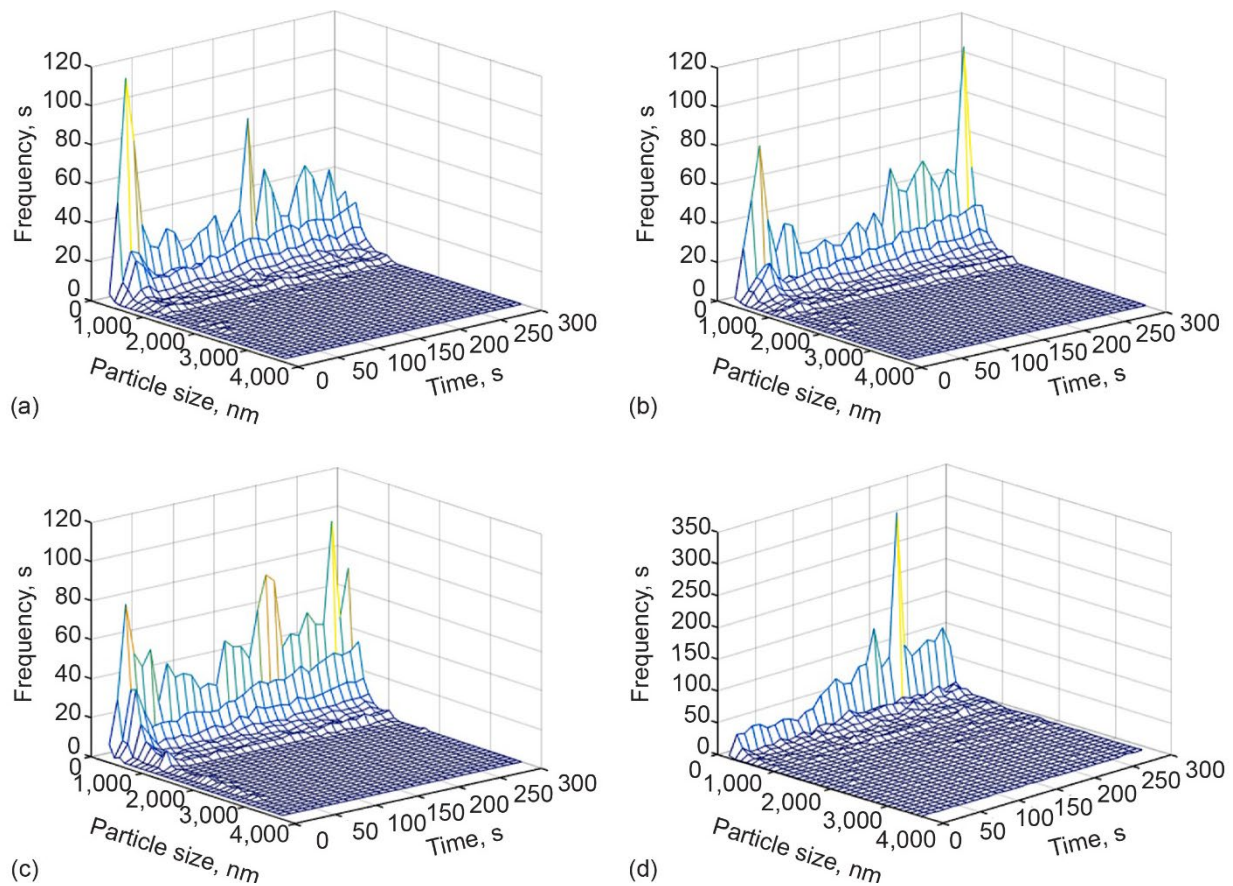


Figure 9.—Average size distributions for all three runs of International Space Station (ISS) hook-and-loop material and Cargo Mission Contract (CMC) sample. (a) ISS Run 1. (b) ISS Run 2. (c) ISS Run 3. (d) CMC sample.

Size Distribution

Particle size distribution data from the laser aerosol spectrometer were recorded every 10 s and varied significantly over the 5-min tests, as shown in Figure 9. Each data set consisting of three replicate tests was averaged and binned by particle diameter, ranging from 100 nm to 10 μm in intervals of 100 nm. The mean frequency of particles larger than 4,000 nm was zero. The data were plotted in three-dimensional graphs to visualize the variation over time. Note that there are periodic spikes in the concentration of the smallest particles in the ISS sample, accompanied by a steady increase in concentration. The frequency scale of the CMC sample plot is much larger, showing a significantly higher population of 100-nm particles.

Particle size distributions captured at 40 s into the tests (Figure 10) have the form of a logarithmic size distribution. Logarithmic distributions can be characterized by the count median diameter (CMD) and the geometric standard deviation (GSD). The arithmetic mean and standard error as well as the CMD and GSD for each run are shown in Table II, which summarizes the parameters of the particle size distributions of the three test runs (all 14 samples). The CMC sample is included as an example of current flight hook-and-loop fasteners. The mean particle sizes and GSDs are remarkably similar, which shows that the VelcroBot provides a repeatable method for testing hook-and-loop emissions. When comparing the number concentration data to the size distribution data, however, it is important to note that the measurement ranges of the two instruments are very different. The WCPC detects particles as small as 5 nm to greater than 3 μm . The laser aerosol spectrometer measures size distribution from 90 nm to 10 μm . It is likely that many particles are below the lower measurement limit of 100 nm (considered ultrafine particles) based on the maximum particle populations consistently residing in the smallest bin.

TABLE II.—PARAMETERS CHARACTERIZING PARTICLE SIZE DISTRIBUTIONS FOR ALL RUNS
 [Mean maximum data from nonreduced, pooled ISS^a test hook-and-loop samples compared with CMC^b sample.]

Parameter	Run 1	Run 2	Run 3	CMC
Particle size diameter				
Mean (x), nm	359.0	352.7	358.0	409.0
Standard error, nm	49.5	48.7	48.9	312.0
Count median diameter (CMD), nm	319.0	313.3	318.8	299.0
Geometric standard deviation (GSD), nm	1.6	1.6	1.6	2.0
Absolute maximum, μm	5.8	5.6	6.0	5.9
Mean maximum, μm	4.6 ± 0.6	4.7 ± 0.7	4.8 ± 0.9	

^aInternational Space Station

^bCargo Mission Contract

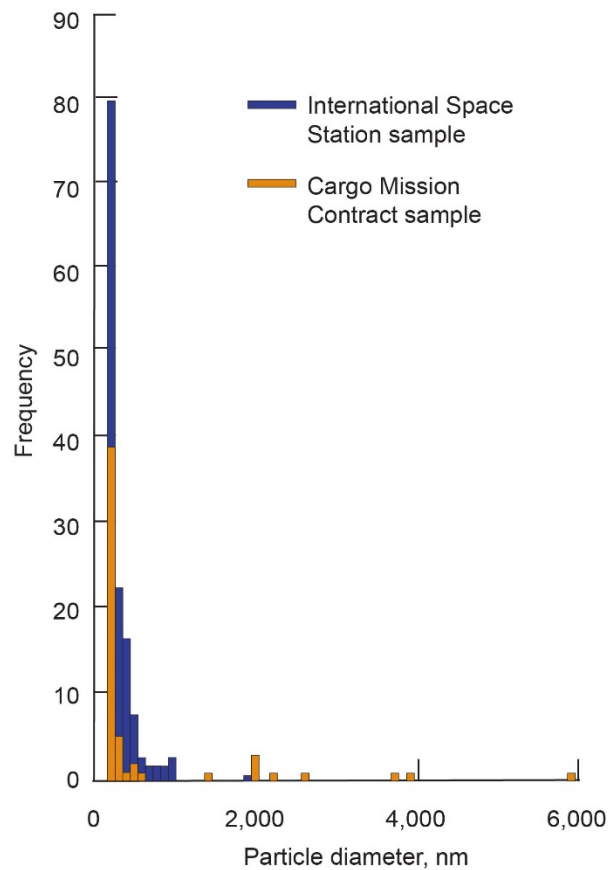


Figure 10.—Comparison of particle size distribution data in Figure 9 at the 40-s mark, showing International Space Station sample Run 1 and Cargo Mission Contract (CMC) hook-and-loop sample.

Electron Microscopy

Electron microscopy was the final technique used to analyze the aerosols emitted from the hook-and-loop fasteners. Two methods of collection were used to prepare samples for microscopy in order to increase the sample set. The TPS100TM aerosol sampler placed inside the test chamber relied on thermophoresis and a flow rate of 0.05 L/min to collect aerosols onto a nickel TEM grid.

The second method of collection relied on the destruction of some ISS hook-and-loop samples that had undergone testing with the VelcroBot and some that had not been tested. The particles observed from these samples cannot technically be classified as aerosols emitted from the hook-and-loop material, but it is expected that the resulting particles on the TEM grid could have become airborne upon mating and demating of the sample pairs. The loops of these samples were cut away from the fastener and placed in ethanol, then sonicated for 5 min to separate particles adhered to the loops. After the loops had settled to the bottom of the beaker, copper grids with lacey carbon were dipped into the suspension, then covered and left to dry. This method of sample preparation was used to study the dark-stained material on one of the samples, shown in Figure 11.

The particles in Figure 12 and Figure 13 were collected from unused ISS hook-and-loop samples (fasteners that had not been mated and demated) and were prepared by the cut-and-wash method. The particles in Figure 14 were collected from the stained ISS samples prepared by the cut-and-wash method. The particle in Figure 15 (inset) was sampled by the TPS100™ during testing of ISS hook-and-loop pieces. The electron microscope was used both in TEM and scanning transmission electron microscopy (STEM) high-angle annular dark field (HAADF) imaging modes. Energy-dispersive spectroscopy (EDS) was used in STEM-HAADF mode, which enabled detection of areas of high atomic number with Z-contrast imaging and partially guided the areas chosen for EDS.

Figure 12 through Figure 15 show the most common particles observed in the microscopic analysis. Zinc oxide flakes and agglomerates were found in all microscopy samples, as shown in the EDS spectrum in Figure 15. The most frequently observed morphology of zinc oxide is shown in Figure 14(a), with zinc oxide flakes in a carbon matrix. This morphology and composition was also the common particle type found most in the stained hook-and-loop sample (Figure 11). Some agglomerates of zinc oxide contained trace amounts of aluminum (Figure 12(a) and (c), Figure 13(a) and (b), and Figure 14(b)). The particle in Figure 12(a), a zinc oxide agglomerate with aluminum, is on the order of 300 nm in diameter. The particle in Figure 13(a), an agglomerate with similar properties, is approximately 200 nm in diameter. A magnified section of this particle is shown in Figure 13(b). The particle in Figure 12(b) is zinc oxide with approximate dimensions of 100 by 250 nm. The particle in Figure 15 (inset) has a long aspect ratio of 525 by 50 nm with embedded zinc oxide flakes (roughly 12 nm in diameter). The particle in Figure 12(c) consists of two zinc oxide and aluminum flakes with diameters of 415 and 350 nm each. The particle in Figure 14(b) is an agglomerate particle roughly 750 by 400 nm with a zinc flake or rod (400 by 40 nm) in its center. Zinc- and aluminum-rich particles are consistent with the 2014 vacuum bag analysis, although no particle size information was reported in that study (Ref. 4).



Figure 11.—Stained sample of International Space Station (ISS) hook-and-loop tape prepared by cut-and-wash method to extract embedded ISS debris particles for transmission electron microscopy (TEM) and scanning transmission electron microscopy (STEM).

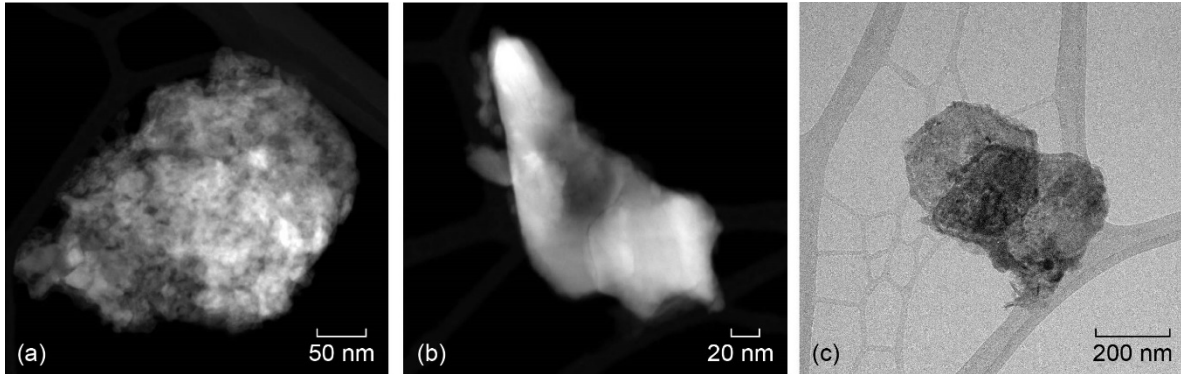


Figure 12.—Zinc oxide in particles from unused International Space Station hook-and-loop samples prepared by cut-and-wash method. (a) Scanning transmission electron microscopy (STEM) image of zinc oxide agglomerate with trace amounts of aluminum. (b) STEM image of sample composed only of zinc and oxygen. (c) Transmission electron microscopy (TEM) image of particle showing two zinc oxide and aluminum flakes.

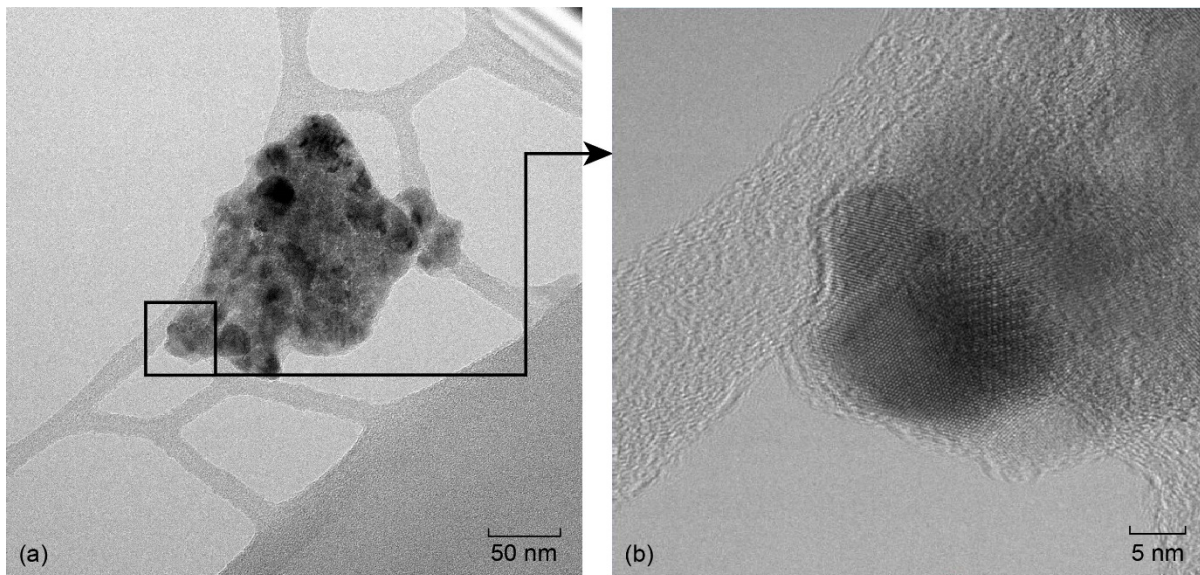


Figure 13.—Particle from unused International Space Station hook-and-loop samples prepared by cut-and-wash method. (a) Transmission electron microscopy (TEM) image of zinc oxide agglomerate with aluminum. (b) Higher magnification of boxed area of (a).

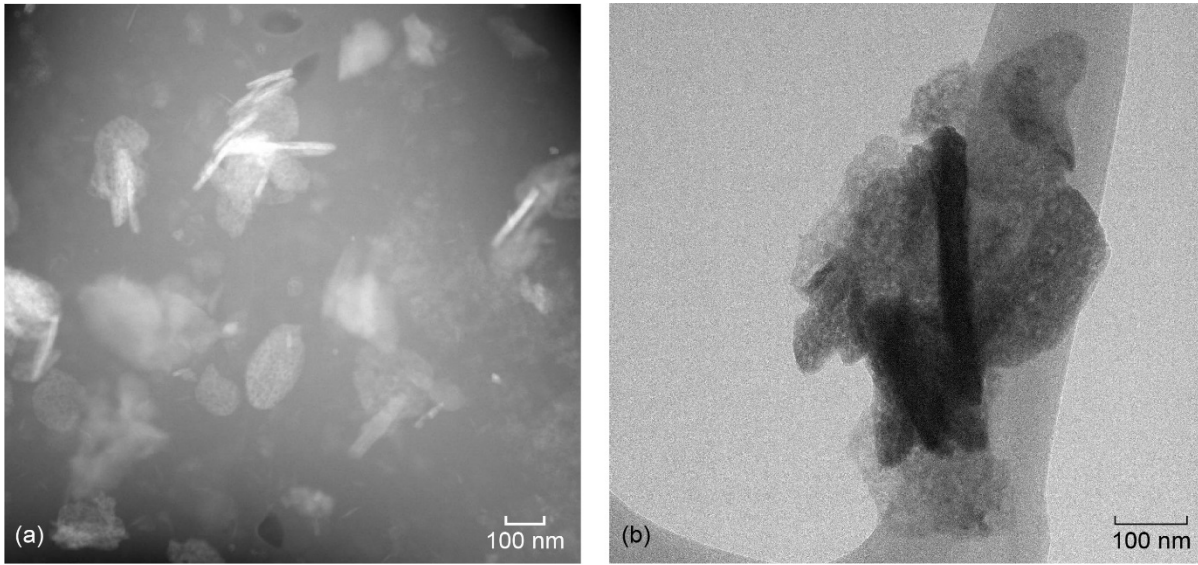


Figure 14.—Stained International Space Station hook-and-loop samples prepared by cut-and-wash method.
 (a) Scanning transmission electron microscopy (STEM) image showing zinc oxide flakes in a carbon matrix.
 (b) Zinc oxide agglomerate with embedded pieces of aluminum.

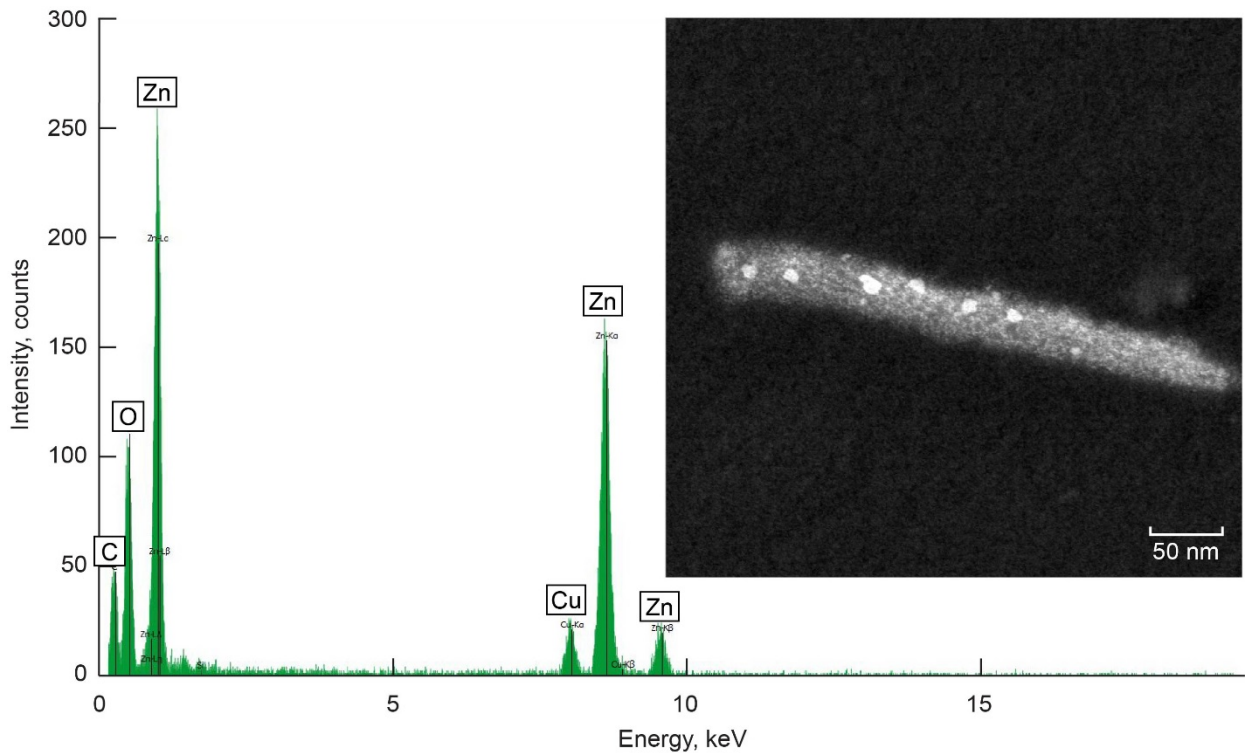


Figure 15.—Typical energy-dispersive spectroscopy (EDS) spectrum representative of all samples (Figs. 12 to 15), with zinc and oxygen peaks. Inset: Scanning transmission electron microscopy (STEM) image of particle with long aspect ratio showing embedded zinc oxide flakes; collected from International Space Station hook-and-loop sample with TPS100™.

Figure 16 and Figure 17 show particles aerosolized by the VelcroBot that were collected with the TPS100™ aerosol sampler. The mating and demating of hook-and-loop pairs produces particles of the native material by mechanical breakdown. Hook-and-loop fasteners are made from semicrystalline polymers such as nylon and polyester, and the EDS spectra of the particles have a prominent carbon peak.

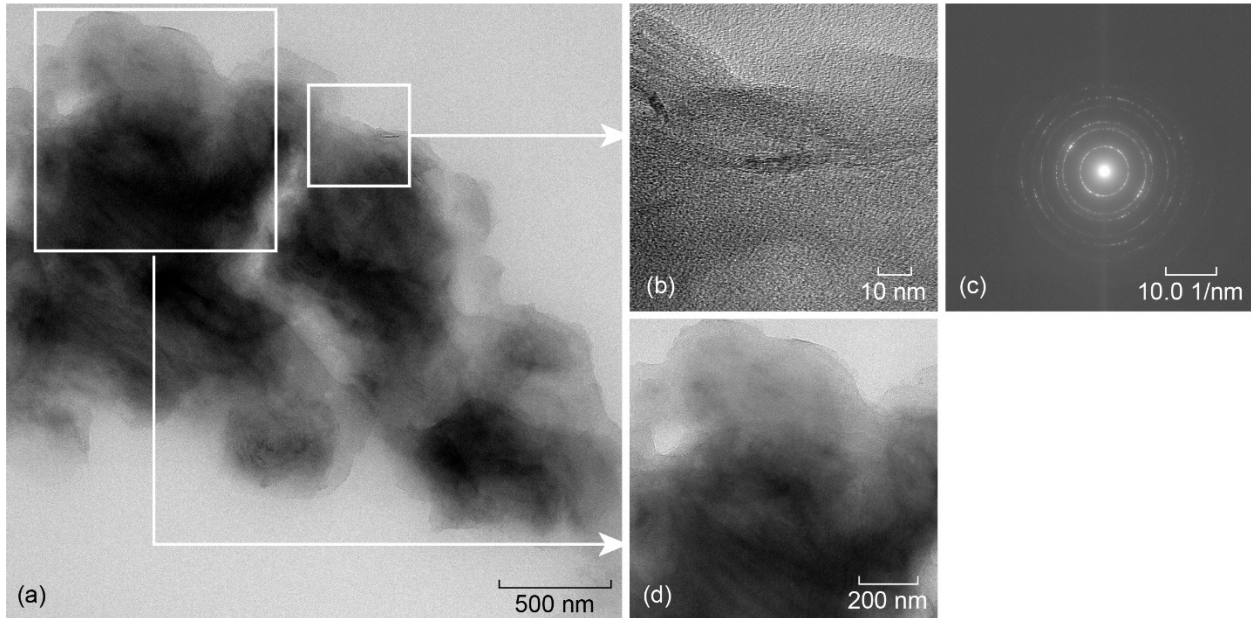


Figure 16.—Aerosolized hook-and-loop particle collected with TPS100™ aerosol sampler. (a) Aerosolized particle. (b) Transmission electron microscopy (TEM) image of magnified section of particle shown in Figure 16(c). (c) Diffraction pattern from location of Figure 16(b). (d) TEM image of another magnified section of Figure 16(a) particle.

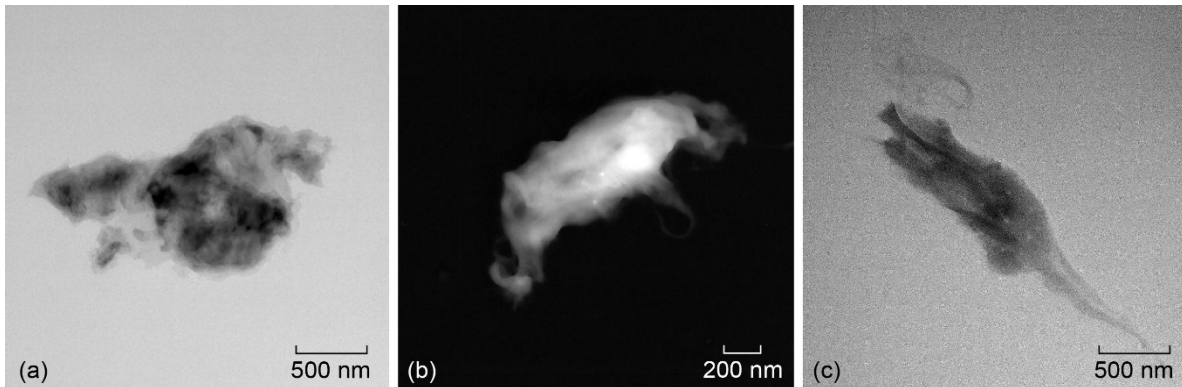


Figure 17.—Aerosolized hook-and-loop particles collected with TPS100™ aerosol sampler. (a) Transmission electron microscopy (TEM) image. (b) Scanning transmission electron microscopy (STEM) image. (c) TEM image.

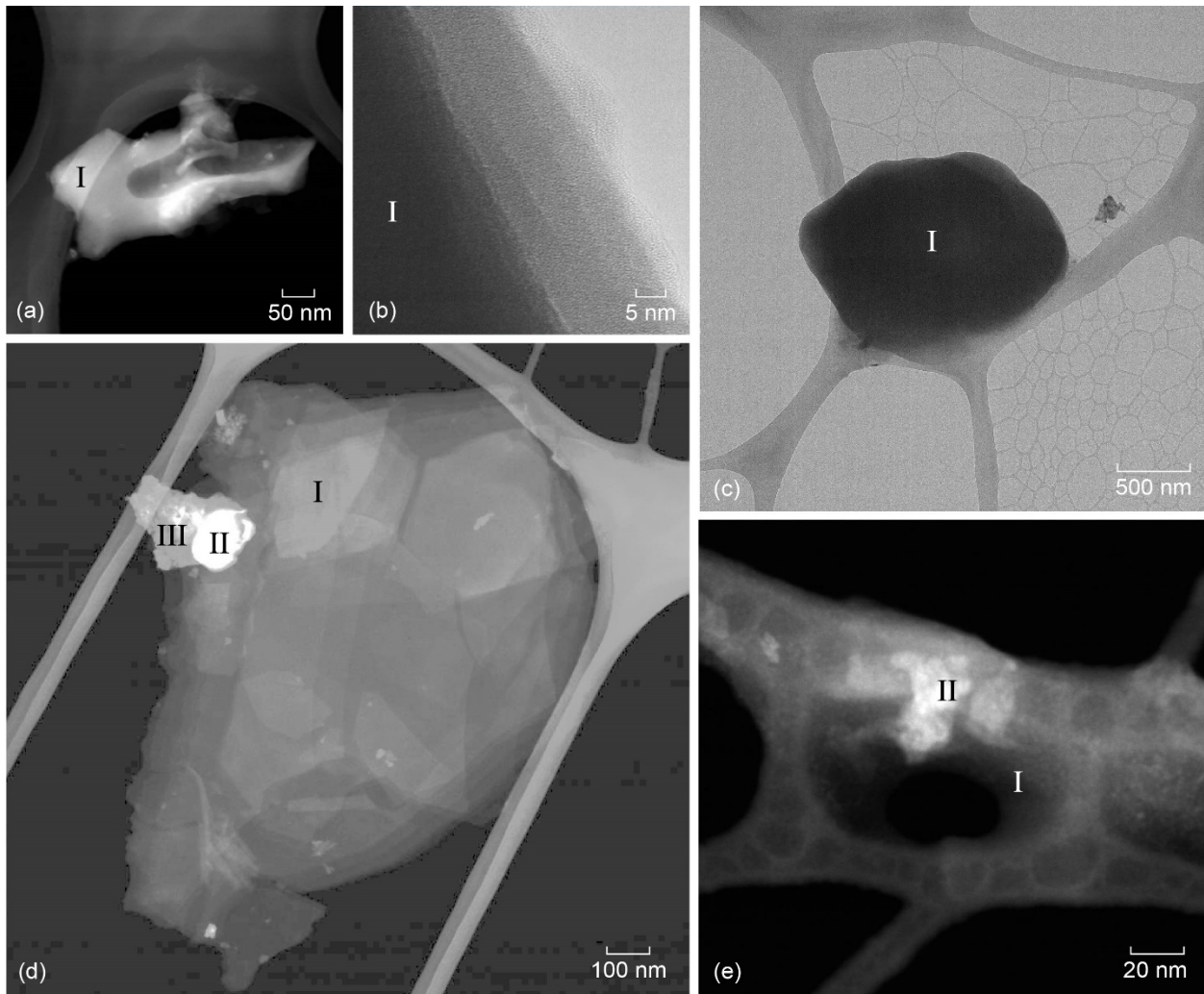


Figure 18.—Silicon- and oxygen-rich particles from International Space Station hook-and-loop pieces that were not mounted to VelcroBot and were collected on transmission electron microscopy (TEM) grid by cut-and-wash method. “I” indicates a particle region high in silicon and oxygen; “II” indicates region rich in zinc and oxygen; “III” indicates a carbon- and oxygen-rich area. (a) Particle composed mostly of silicon and oxygen. (b) Particle closeup showing amorphous structure. (c) Particle composed of amorphous silicon and oxygen. (d) Particle in scanning transmission electron microscopy (STEM) mode showing three distinct regions. (e) Silicon- and oxygen-rich particle with region containing zinc and oxygen.

Figure 18 shows examples of particles that are rich in silicon and oxygen. The particles in Figure 18(a) and (c) have amorphous structure, such as that seen in Figure 18(b). Some particles in this class had agglomerated or embedded regions with zinc (Figure 18(d) and (e)). The particle in Figure 18(a) is roughly 400 by 200 nm, composed mostly of silicon and oxygen, with trace amounts of sulfur, calcium, potassium, and zinc. The particle in Figure 18(c) is amorphous silicon and oxygen, roughly 1800 by 1400 nm. The STEM image in Figure 18(d) shows a particle with three distinct regions. EDS revealed silicon and oxygen in the large, light gray areas, designated by “I”; zinc and oxygen in the white areas, designated by “II”; and a carbon-rich region with traces of oxygen, sulfur, and potassium, designated by “III.” Figure 18(e) shows a silicon- and oxygen-rich particle with a region containing zinc and oxygen embedded within it, designated by “II.”

The stained hook-and-loop portion in Figure 11, which was sampled on the TEM grid by the cut-and-wash method, had an agglomerate on the lacey carbon of the TEM grid, shown in Figure 19. The primary

particle sizes range from 50 to 100 nm and cover a net area of 17,880 nm². The EDS analysis of the elemental composition of these particles is shown in Figure 19(c). This particle agglomeration is a good example of the variety of elements seen throughout the microscopic analysis, including carbon, oxygen, zinc, aluminum, sulfur, potassium, and calcium, with the copper peak attributed to the TEM grid.

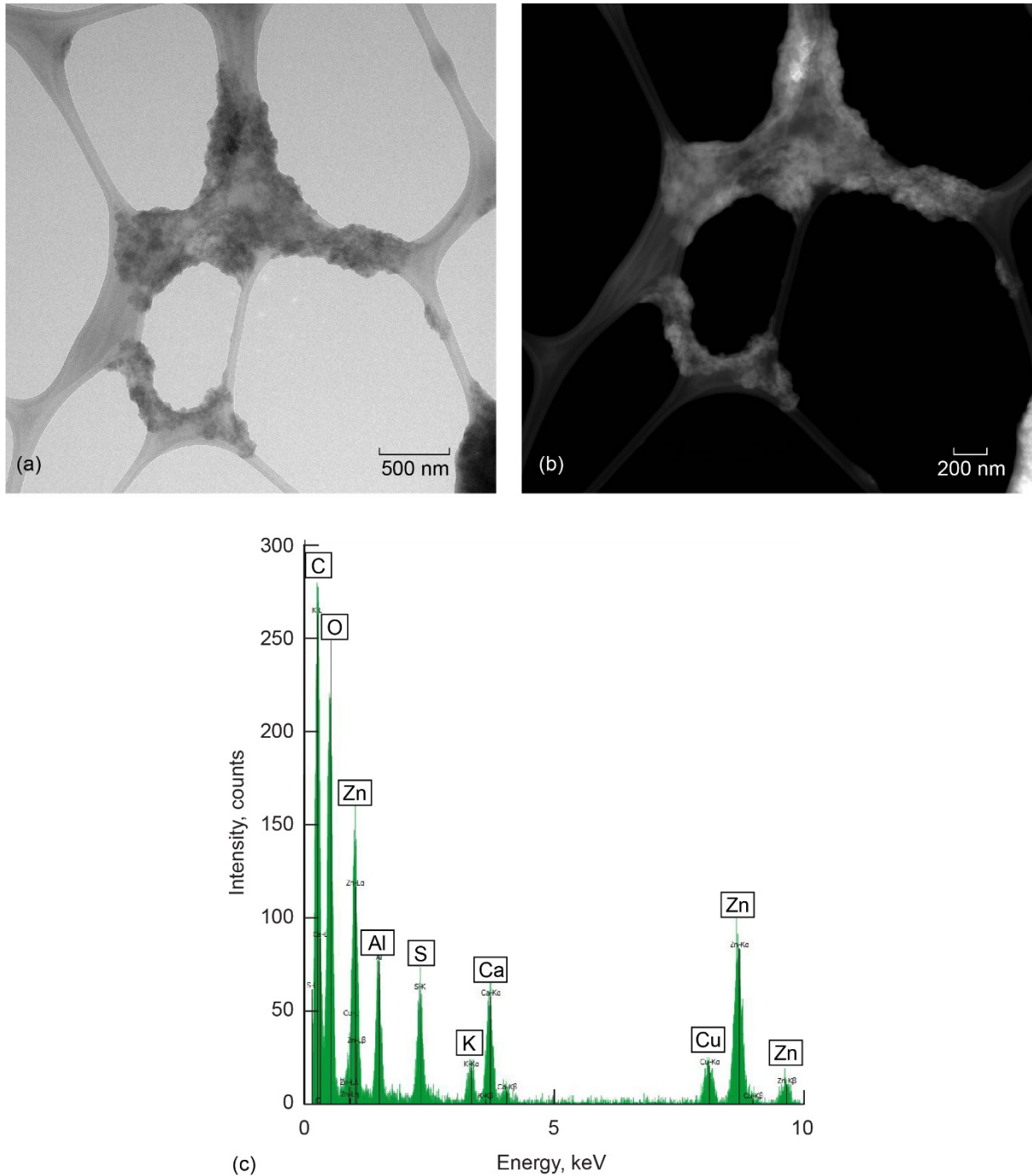


Figure 19.—Particles from stained portion of International Space Station hook-and-loop material collected on transmission electron microscopy (TEM) grid by cut-and-wash method show an agglomerate with primary particles ranging from 50 to 100 nm. (a) Agglomerate in TEM mode. (b) Agglomerate in scanning transmission electron microscopy (STEM) mode. (c) Energy-dispersive spectroscopy (EDS) spectrum showing zinc, aluminum, silicon, potassium, calcium, oxygen, and carbon in addition to copper from TEM grid.

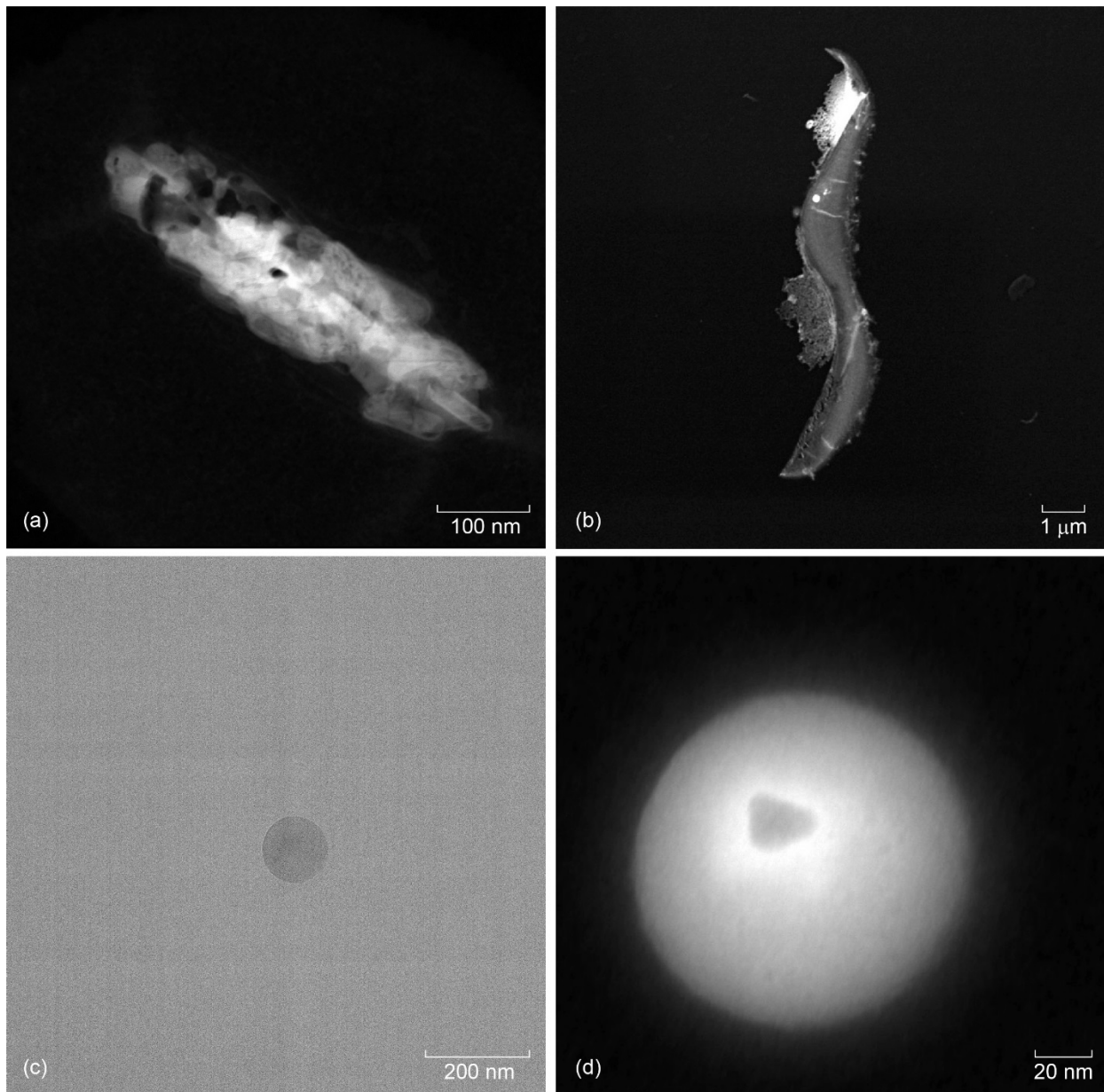


Figure 20.—Scanning transmission electron microscopy (STEM) and transmission electron microscopy (TEM) images of unique particles collected with TPS100™ aerosol sampler. (a) Agglomerate of rod-like particles, possibly of biological origin. (b) Largest particle seen. (c) Spherical particle shown in TEM mode. (d) Closeup of spherical particle shown in STEM mode.

Figure 20 shows particles generated by the cut-and-wash method that have either unusual morphology or sensitivity under the electron beam. The particle in Figure 20(a) is an agglomerate of rod-like particles, with two of the rods in the lower right of the micrograph measuring approximately 80 by 20 nm and 90 by 30 nm. The black dot in the center and several other dark spots were caused by damage from the electron beam. Upon further focusing in STEM mode, the particle began to degrade under the intensity of the electron beam. Beam sensitivity and the rod-like morphology suggests that this particle may be of biological origin. The particle in Figure 20(b) was the largest particle seen, measuring 11 by 1 μm. The

EDS area scan shows carbon, oxygen, and silicon, and the bright white particle toward the middle of the sample is calcium and oxygen with trace amounts of silicon. Other areas contain trace amounts of aluminum. This particle did not deteriorate when subjected to the electron beam.

Many spherical particles were found throughout the grid, one of which is shown in TEM mode (Figure 20(c)) and STEM mode (Figure 20(d)). The sphere has a diameter of 125 nm and consists of potassium. The image in Figure 20(d) has a dark spot in its center, which is a result of damage by the electron beam.

Inhaled Particle Lung Deposition in Low Gravity

There are three modes of aerosol deposition in the lung: impaction, sedimentation, and diffusion. Brownian motion drives diffusion, while impaction is driven by the inertial properties. Sedimentation, the only gravity-dependent process, is absent on the ISS (Ref. 8). For particles greater than 500 nm, inertial properties dictate the site of deposition (Ref. 7), and diffusion dominates below this size.

Several studies have been conducted regarding the site of aerosol deposition in the human lung as a function of gravity and particle size. In low gravity, sites of lung deposition and amount of deposition are different from what is observed on Earth. A study by Darquenne et al. has shown that deposition of particles between 500 nm to 3 μm in microgravity is underestimated by one-dimensional models (Ref. 9). When gravitational settling is absent, the concentration of particles in the airways is higher and thus enhances particle transport to the alveolar region.

Toxicological effects of inhaled particles vary widely and depend on particle size, material composition, morphology, and surface area, as well as deposition location and how quickly particles can be removed. Particles deposited in the head and lung airways are cleared relatively quickly by mucociliary transport; however, particles deposited in the alveolar region of the lungs remain longer, as this region has no mucociliary clearance mechanism. Clearance from the alveolar region of the lung is driven by phagocytosis due to macrophages, so the clearance rate is on the order of months to years. The hook-and-loop particle emissions in this study were mostly below 500 nm, a size for which Brownian diffusion is a significant lung deposition mechanism. On Earth, the deposition of these particles would be predominantly in the intermediate and peripheral regions of the lung (Ref. 10). Further study is needed to understand the lung deposition sites of inhaled particles in low gravity, particularly for particles smaller than 2 μm .

Conclusions

This study successfully characterized particles emitted from repeatable mating and demating of hook-and-loop fasteners and generated aerosols from the International Space Station in an Earth-based laboratory by virtue of a returned set of fasteners that had been in use on the Microgravity Science Glovebox. With mass concentration, number concentration, and size distribution findings, we have confirmed hook-and-loop fasteners as both a source and a sink of aerosol particles, demonstrated that their use creates localized pollution, and provided the base numbers through which the health effects of these fasteners can begin to be explored. It would be beneficial to test such fasteners for aerosol emission properties before selection for use in spacecraft or, better yet, to consider an alternative fastener material that does not create aerosols.

References

1. Spivey, Reggie A.; Sheredy, William A.; and Flores, Ginger: An Overview of the Microgravity Science Glovebox (MSG) Facility, and the Gravity-Dependent Phenomena Research Performed in the MSG on the International Space Station (ISS). AIAA-2008-812, 2008.
2. NASA Space Flight Human-System Standard. Volume 2: Human Factors, Habitability, and Environmental Health, NASA-STD-3001, Vol. 2A, 2015.
<https://standards.nasa.gov/standard/nasa/nasa-std-3001-vol-2> Accessed Aug. 6, 2018.
3. Perry, J.L.: International Space Station Bacteria Filter Element Service Life Evaluation. NASA/TM—2005-213846, 2005. <http://ntrs.nasa.gov>
4. Perry, Jay L.; and Coston James E.: Analysis of Particulate and Fiber Debris Samples Returned From the International Space Station. ICES-2014-166, 2014.
5. Meyer, Marit: ISS Ambient Air Quality: Updated Inventory of Known Aerosol Sources. ICES-2014-199, 2014.
6. Leith, David, et al.: Development of a Transfer Function for a Personal, Thermophoretic Nanoparticle Sampler. *Aerosol Sci. Technol.*, vol. 48, no. 1, 2014, pp. 81-89.
7. Brown, James S., et al.: Thoracic and Respirable Particle Definitions for Human Health Risk Assessment. *Part. Fibre Toxicol.*, vol. 10, no. 12, 2013.
8. Darquenne, Chantal: Aerosol Deposition in the Human Lung in Reduced Gravity. *J. Aerosol Med. Pulm. Drug Deliv.*, vol. 27, no. 3, 2014, pp. 170-177.
9. Darquenne C., et al.: Effect of Microgravity and Hypergravity on Deposition of 0.5- to 3- μ m-Diameter Aerosol in the Human Lung. *J. Appl. Physiol.*, vol. 83, no. 6, 1997, pp. 2029-2036.
10. Martonen, T.B.; and Katz, I.: Deposition Patterns of Polydisperse Aerosols Within Human Lungs. *J. Aerosol Med.*, vol. 6, no. 4, 2009, pp. 251-274.

